Journal of Construction and Engineering Technology
Journal homepage: www.journal.fstu.uz

ANALYSIS OF THE RELATIONSHIP BETWEEN WATER CONSUMPTION AND HEADIN A MICRO HYDROPOWER SYSTEM

Uktam Salomov, Akmaljon Kuchkarov, Omadjon Urishev

Fergana State Technical University
*Correspondence: orishevomadjon@gmail.com

Abstract

This study analyzes the relationship between water consumption and head losses in a micro hydropower system, with a particular focus on penstock hydraulics. Using mathematical modeling combined with computational fluid dynamics (CFD), the research evaluates the effects of varying water flow rates on velocity distribution, pressure loss, and head efficiency. Results indicate that velocity magnitude increases proportionally with flow rate, with peak values reaching 9.4 m/s at 3 m^3/s. Pressure distributions demonstrate that head losses are strongly dependent on flow rate and pipe geometry, confirming the quadratic relationship between velocity and frictional resistance. The findings emphasize the importance of optimal pipe diameter selection and accurate modeling of both friction and minor losses, especially under transitional and turbulent flow conditions. This study provides insights for the efficient design of micro hydropower systems, ensuring stable turbine operation, reduced hydraulic losses, and improved energy output.

Keywords: Micro hydropower, head loss, pipe hydraulics, water consumption, penstock, CFD modeling, renewable energy.

Introduction

Today, the global demand for clean and renewable energy sources continues to increase, driven by concerns over climate change, fossil fuel depletion, and the need for sustainable energy access. This issue is particularly critical for rural communities and agricultural areas located far from centralized power grids. For such locations, micro-hydropower plants (MHPs) represent a cost-effective and environmentally friendly solution capable of providing decentralized electricity generation.

A micro-hydropower plant is a small-scale hydroelectric installation that converts the kinetic and potential energy of flowing water into electrical energy, typically with a power capacity of up to a few megawatts. These systems can be deployed on rivers, irrigation canals, or small natural streams. Micro-hydropower plants offer several advantages, including low operational and environmental costs, independence from fossil fuel supply chains, resilience to changing weather conditions, and the ability to deliver continuous energy to remote regions. Moreover, they play an important role in reducing greenhouse gas emissions and promoting sustainable development.

The efficient operation of a micro-hydropower plant largely depends on key hydraulic parameters—namely, water discharge (Q), head (H), and flow velocity. Among these factors, head losses occurring in the penstock or transmission pipeline have a significant influence on the overall system efficiency. These losses depend on the pipe's length, diameter, surface roughness, and flow turbulence level. Therefore, their accurate estimation and analysis are essential for the proper design and optimization of hydropower systems.

Head losses are defined as the energy losses due to frictional forces and geometric irregularities encountered by the water as it flows through the pipeline. They can vary considerably depending on the flow regime (laminar, transitional, or turbulent) and the roughness of the pipe surface. The general equation proposed by Avci and Karagoz [1] allows accurate calculation of water head losses under various flow conditions, enabling more precise hydraulic modeling for micro-hydropower projects. Analytical studies show that in pipelines located close to the water intake, flow velocity has a stronger influence on head losses, whereas in the downstream sections, pipe diameter becomes the dominant factor. This highlights the

Received: 6 September 2025
Revised: 11 September 2025
Accepted: 23 October 2025

https://doi.org/10.24412/2181-4473-2025.3.204

necessity of carefully selecting the pipeline geometry according to its position within the system.

In determining water head losses, not only major losses caused by friction but also minor losses—which occur at bends, valves, bifurcations, and cross-sections—play a crucial role. These localized losses are often evaluated using the loss coefficient (K) [2]. However, the constant K values applied in many engineering calculations are valid primarily for fully developed turbulent flow. In micro-hydro systems, where discharge rates are relatively low, the flow may instead be laminar or transitional, resulting in higher relative local losses. In such cases, the K-coefficient must be corrected based on the Reynolds number, as demonstrated by several studies [3].

In recent years, growing research attention has been devoted to the numerical modeling of penstock systems in order to better understand their complex hydraulic and structural behavior. The advancement of Computational Fluid Dynamics (CFD) has enabled a detailed investigation of internal flow phenomena, including pressure distributions, velocity fields, and the risk of cavitation or structural failure under varying operational conditions. Among modern simulation platforms, COMSOL Multiphysics, which employs the finite element method (FEM), offers a versatile and integrated framework for conducting coupled fluid flow and solid mechanics analyses [4].

Several researchers have applied CFD-based methodologies to investigate the flow dynamics and stability of complex penstock configurations. For instance, Xinran Guo et al. (2019) conducted a detailed CFD analysis of hydropower stations equipped with multi-turbine division systems connected by a common penstock. Using ANSYS Fluent, the authors demonstrated that vortex-induced pressure oscillations at the trifurcation section were the main source of instability in power generation. Their study further revealed that incorporating guide plates effectively reduced flow separation, mitigated pressure fluctuations, and enhanced the overall stability of the system. Moreover, the authors recommended adopting a smaller inlet-to-branch diameter ratio and higher outlet flow velocities to improve hydraulic and operational performance [5].

Building upon these findings, subsequent studies have aimed to overcome the limitations of conventional CFD approaches in modeling transient hydraulic behavior and fluid–structure interaction (FSI) within penstock systems. While traditional CFD methods can effectively simulate steady-state flow characteristics, they often struggle to capture unsteady transient events such as water hammer, pressure surges, and elastic deformations of the pipeline under fluctuating loads. These dynamic processes require strongly coupled FSI models that account for two-way interactions between the fluid domain and the structural response.

Recent progress in multiphysics simulation frameworks, particularly within COMSOL Multiphysics, has made it possible to couple the Navier–Stokes equations with solid mechanics equationtions, thereby providing a more realistic representation of penstock behavior under real operating conditions. This integrated modeling approach enables detailed analysis of stress concentrations, vibration modes, and fatigue life of pipeline materials subjected to hydraulic loading. Additionally, such models offer insights into how geometric design, boundary conditions, and turbulent flow regimes affect the overall hydraulic stability and structural integrity of hydropower systems.

Nevertheless, further refinement in mesh optimization, turbulence modeling, and computational efficiency is still required to enhance simulation accuracy without excessive computational cost. The use of adaptive meshing techniques, transient turbulence models, and high-performance computing (HPC) tools can significantly improve the fidelity and scalability of CFD–FSI simulations. Consequently, contemporary research continues to focus on developing integrated numerical frameworks that can accurately reproduce complex flow phenomena and serve as reliable design tools for optimizing penstock geometry, material selection, and operating parameters in micro-hydropower applications.

Therefore, this study investigates the interdependence between water discharge, head, and head losses in a micro-hydropower system. The primary objective is to model pressure variations along the transmission pipeline, quantify hydraulic losses, and evaluate their influence on the overall energy conversion efficiency of the system.

2. Materials and Methods

The numerical investigation of hydraulic behavior within the penstock system was carried out using Computational Fluid Dynamics (CFD) techniques. The methodology adopted in this study involves a sequence of stages, including geometric modeling, mesh generation, boundary condition specification, solver setup, and post-processing analysis. The primary objective was to evaluate flow characteristics, pressure distribution, and potential cavitation zones under different operational scenarios.

The three-dimensional model of the penstock was developed based on the actual geometric dimensions of a medium-scale hydropower plant configuration. The model includes the main conduit, bifurcation/trifurcation section, and turbine inlet zone. To ensure numerical accuracy and stability, the computational domain was discretized using an unstructured mesh with local refinement in regions expected to exhibit strong velocity gradients or vortex formations. The finite volume method (FVM) was employed to solve the governing Navier–Stokes equations for incompressible, turbulent flow.

Turbulence effects were modeled using the Reynolds-Averaged Navier–Stokes (RANS) approach with the k–ε turbulence model, which provides a good balance between computational efficiency and accuracy for internal flow applications. Boundary conditions were set as follows: the inlet was defined by a prescribed mass flow rate or velocity profile, while the outlet was assigned a static pressure condition corresponding to turbine operation. The no-slip condition was applied along all wall surfaces.

The power generated in a micro hydroelectric power plant is calculated using the equation.

$$P = \rho \cdot g \cdot Q \cdot H_n \cdot \eta_g \cdot \eta_t \quad (1)$$

Where: P - Power output (kW), Q - water flow rate (m^3/s), g - gravitational acceleration (m/s^2), H_n- Head (m), η_t −Turbine efficiency, for a Kaplan turbine is usually 85-93% [6]. According to the practical results of the generator manufacturer and the analysis of the literature, the efficiency of a permanent magnet generator with a frequency of 50 Hz usually exceeds 95% [7, 8].

The water pipe supplies the turbine with water under pressure due to the height of the gate. It is preferable to supply the turbine with water pipes over short distances [9]. The effective diameter of the water pipe for the turbine (m) is calculated using the following equation [8]:

The following dimensions characterize it:

$$D_P = 2.69\left(n_P^2 \cdot Q^2 \cdot \frac{L_P}{H_n}\right) \quad (2)$$

Here, np is the manning coefficient, Q is the turbine water flow rate (m^3/s), Lp is the water transfer pipe length (m), and Hn is the head (m).

The wall thickness of the water pipe depends on the pipe material, its tensile strength, pipe diameter and working pressure. The minimum wall thickness is recommended by the following equation:

$$t_P = \frac{D_P+508}{400} + 1.2 \quad (3)$$

Where: D_P-water pipe diameter (mm), tp-minimum water pipe thickness (mm).

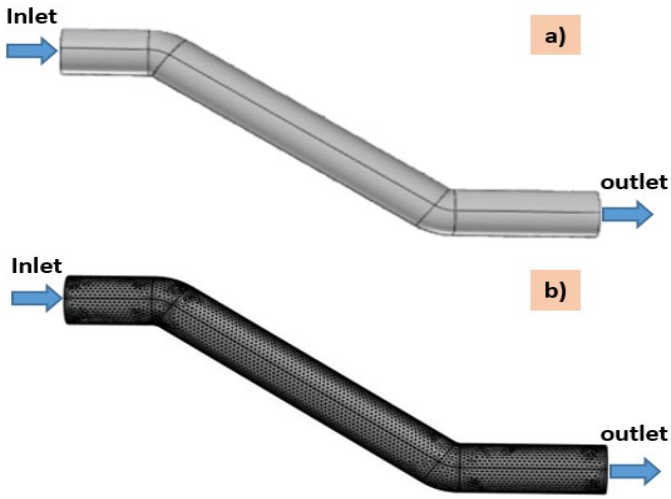


Fig. 1. a) Geometric view of the penstock of hydropower systems, b) generated mesh size for penstock of hydropower systems.

Here (Figure 1), the computational domain was discretized using a free tetrahedral mesh, with locally refined elements near the pipe wall to accurately capture boundary layer effects. A mesh independence study was conducted by testing three different grid densities containing approximately 0.5 million, 1.0 million, and 2.0 million elements. When the difference in pressure loss results between successive refinements was less than or equal to 1%, the mesh with 1.0 million elements was selected as optimal. This configuration provided a good balance between computational efficiency and solution accuracy.

The diameter of the water supply pipe was determined using equation (2). The total pressure loss in the transfer pipeline is calculated using the following equation [11]:

$$\sum \Delta h = \Delta h + h_q \quad (4)$$

Here: $\sum \Delta h$- total water head loss in the transfer pipe, Δh - head loss due to friction in the water path in the transfer pipe, h_q- water head loss due to hydraulic resistance created by the bend in the transfer pipe.

There are three different approaches to determining pressure loss in a water pipeline, including the Manning, Hazen Williams, and Darcy-Weisbach equations. Manning's equation is typically used for open channels and relates the velocity of the fluid in the open channel to the properties of the open channel.

$$Q = \frac{A}{N} R_h^{2/3} S^{1/2} \quad (5)$$

Where: Q- water flow (m³/s), R_h - hydraulic radius (m), calculated by $R_h = A/P$, A- flow passage surface (m²), P- wetted surface perimeter (m), S- slope, N- Mann's coefficient is a function of the channel material.

Mann's equation is an empirical equation that applies to uniform flow in open channels and depends on the flow velocity, flow area, and channel slope. Using the Darcy-Weisbach equation, finding the v-flow velocity in an open channel is given by equation (5).

$$v = \frac{1}{N} R_h^{2/3} S^{1/2} \quad (6)$$

The Hazen Williams equation is typically used in systems with small water flow rates, with pipe diameters d ≥ 50 mm and water velocities v ≤ 3 m/s.

The Hazen Williams equation for determining Headloss in a transfer pipe is given below.

$$h_L = 10.626 \frac{L}{C^{1.85} d^{4.87}} Q^{1.85} \quad (7)$$

Where: h_L-head loss in the transfer pipe, Transfer pipe length, C- Hazen Williams roughness coefficient according to table 1, d-internal diameter of the transfer pipe.

Table 1. The coefficient of roughness for different materials.

Material	Manning coefficient N	Hazenh-Williams coefficient C	Darcy-Weisbach roughness index, ε (mm).
Asbestos cement	0.011	140	0.0015
Brass	0.011	135	0.0015
Brick	0.015	100 ..	0.6
Iron, new	0.012	130	0.26
Concrete:			
Steel shapes	0.011	140	0.18
Wooden shapes	0.015	120	0.6
Centrifugal forms	0.013	135	0.36
Copper	0.011	135	0.0015
Corrugated metal	0.022	-	45
Galvanized iron	0.016	120	0.15
Glass	0.011	140	0.0015
Lead	0.011	135	0.0015
Plastic	0.009	150	0.0015
Steel			
Charcoal coated	0.010	148	0.0048
Without a new line	0.011	145	0.045
Riveted	0.019	110	0.9

The flow rate inside the transfer pipe can be calculated using the Hazen Williams equation.

$$v = 0.355 C d^{0.63} S^{0.54} \quad (8)$$

Using the Darcy-Weisbach equation and the Moody friction coefficient, it is possible to calculate the flow parameters and pressure loss in many types of water pipes [10]. As we have seen above, unlike the Hazen Williams, Manning equation, the Darcy-Weisbach equation does not have any limitations on water flow rate and pipe diameter and is suitable for closed transfer pipes, so it is possible to calculate the pressure loss for a micro hydropower water transfer pipe.

$$h_L = f \frac{L}{D} \frac{V^2}{2g} \quad (9)$$

Here: v-average water flow velocity (m/s), D - water pipe diameter (m), h_L- length is the pressure loss (m), f- Moody friction factor (dimensionless empirical factor, Reynolds number and ε/D function where ε is the roughness index According to figure 2.

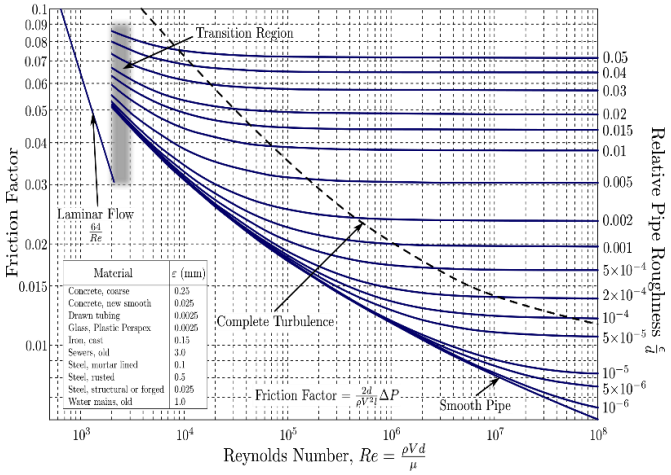


Figure 2. Moody diagram showing the Darcy Weisbach roughness index.

Here (figure 2) the Moody diagram is used to determine the friction factor needed to compute pressure losses in pipe flow, based on whether the flow is laminar, transitional, or turbulent, and depending on the pipe's roughness.

Moody friction factor f value Darcy Weisbach for calculations with the equation, it is necessary to measure all the other parameters in the equation, and a common way to obtain the value of f is the Moody friction factor diagram [13,14].

Moody friction factor f value Darcy Weisbach for calculations with the equation, it is necessary to measure all the other parameters in the equation, and a common way to obtain the value of f is the Moody friction factor diagram (figure 2) [14].

Water flow can be laminar or turbulent, depending on factors such as the inlet conditions and the roughness of the pipe surface. Based on Reynolds experiments and subsequent measurements, the now

widely accepted criteria are that pipe flow is laminar when the Reynolds number (*Re*) is less than 2100, 2100 < *Re* < 4000 in the transition region, and turbulent when it is greater than 4000.

The Reynolds number for flow in pipes is defined as:

$$R_e = \frac{DV\rho}{\mu} \quad (10)$$

Where: ρ-density of the liquid in the pipe (kg/m3), μ-viscosity of the fluid inside the pipe (Ns/m²) (table 2).

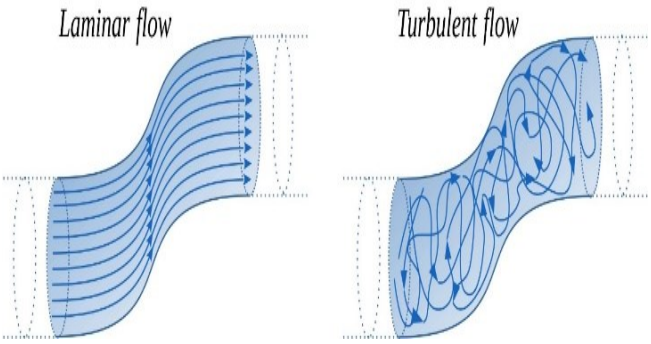


Figure 3. Differences in Reynolds numbers between laminar and turbulent flow in a pipe.

The Reynolds number for flow in pipes is defined as

$$R_e = \frac{DV\rho}{\mu} \quad (11)$$

Where: ρ-density of the liquid in the pipe (kg/m³), μ-viscosity of the fluid inside the pipe (Ns/m²).

Table 2. The dependence of water viscosity on temperature

Water temperature (C^0)	Water viscosity. (mPa.s)
5	1.5182
10	1.3059
15	1.1375
20	1.0016
25	0.89
30	0.7972

The flow of water or air in a pipeline is usually turbulent. Laminar flow occurs with fluids of high viscosity.

The Moody friction factor and Re for the 4 different parts of the Moody diagram (Figure 2). There are equations that give the relationship between ε/D.

The equations for these four parts are shown as follows:

The flow of water or air in a pipe is usually turbulent. Laminar flow occurs with fluids of high viscosity. The Moody friction factor and R_e there are equations that give the relationship between ε/D. The equations for these four parts are as follows:

Moody friction factor for laminar flow Re < 2100 - straight line on the left side of the Moody diagram):

$$f = \frac{64}{R_e} \quad (12)$$

ε=0 (ideally smooth) for turbulent flow Moody friction factor:

$$f = \frac{0.316}{R_e^{1/4}} \quad (13)$$

Moody friction factor for completely turbulent flow:

$$f = [1.14 + 2\log_{10}(\frac{D}{\varepsilon})]^{-2} \quad (14)$$

Moody friction factor for the flow transition area:

$$f = \{-2\log_{10}[\frac{\left(\frac{\varepsilon}{D}\right)}{3.7} + \frac{2.51}{R_e\left(f^{\frac{1}{2}}\right)}]\}^{-2} \quad (15)$$

The head loss due to hydraulic resistance caused by the bend in the transfer pipe can be calculated using the following equation:

$$h_q = \xi\frac{V^2}{2g} \quad (16)$$

Here: $\xi -$ resistance coefficient (according to Appendix 1). Change in pressure loss depending on water consumption when the diameter of the water supply pipe is constant D (0.8m).

3. Results

Here, the topographic map data and optical theodolites, where the H_n-head is measured, and can be determined using a device operating via the Global Navigation Satellite System (GNSS).

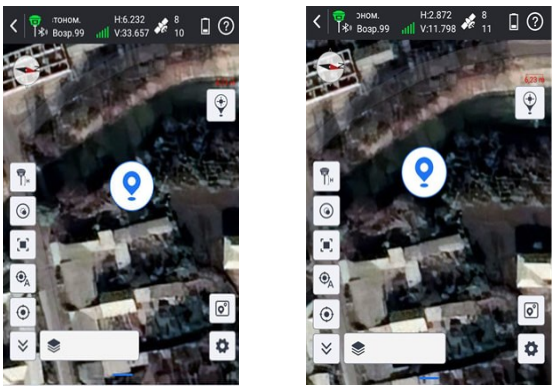


Figure 4. Geospatial survey taken at the Kolida K7 facility to determine head for the installation of a micro hydropower plant.

Here (figure 4) a geospatial survey was conducted using the Kolida K7 GNSS facility to determine the water head and elevation differences along the flow channel. The survey aimed to obtain high-precision topographic data necessary for evaluating the hydraulic gradient and potential energy distribution

within the system. Field measurements were taken at key upstream and downstream locations using differential GNSS positioning with centimeter-level accuracy. The collected elevation data were processed and referenced to a local geodetic datum to ensure consistency and reliability. The resulting elevation profile was then used to compute the water head (H_n) as the difference between the hydraulic elevations at two points, providing essential input for subsequent flow and energy loss analyses.

The simulation will use the Turbulent Flow, *k-e* interface, which is well known for modeling high-Reynolds-number flows. The results will shed light on velocity distribution, pressure drop, and flow behavior under different inlet conditions. This work will contribute to design optimization and enhance the reliability of hydropower systems.

The flow behavior in the micro hydroelectric turbine was modeled using the Reynolds-Averaged Navier–Stokes (RANS) equations combined with the standard k–e turbulence model. These governing equations describe the conservation of mass and momentum for an incompressible turbulent fluid.

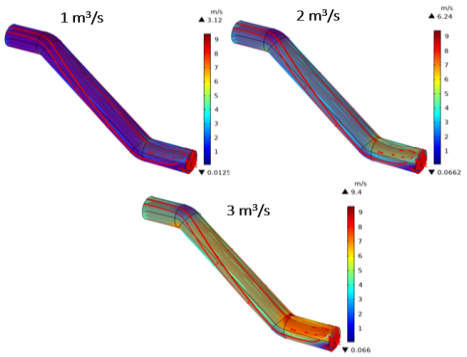


Figure 5. Velocity contours for various flow rates in the channel

As expected, the velocity magnitude rises with the flow rate. Peak velocities are around 3.12 m/s, 6.24 m/s and 9.4 m/s, for flow rates of 1 m³/s, 2 m³/s and 3 m³/s, respectively.

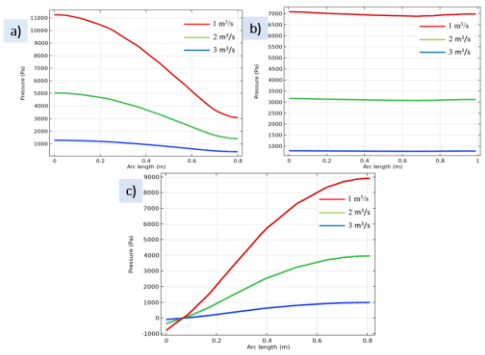


Figure 6. Pressure variation of penstock of hydropower systems at three different Cut lines, a) Cut line at inlet section, b) Cut line at middle section, c) Cut line at outlet section.

Pressure distributions along the pipe arc length at different flow rates (1, 2, and 3 m³/s). Subfigure (a) shows a significant pressure drop along the pipe due to frictional resistance, (b) illustrates relatively stable pressure conditions, and (c) indicates pressure rise under specific boundary conditions. The results demonstrate that pressure losses, and therefore head loss, increase with flow rate, consistent with the quadratic relationship between velocity and frictional losses in pipe flow.

Table 3. Variation of pressure loss depending on water consumption when the diameter of the water supply pipe is constant D (0.8m).

Q (m^3/s)	h_L (m)	V (m/s)	Re	f (turf)	f (grass)
0.4	0.003	0.79	486 003	0.01517	0.0165
0.6	0.009	1.18	727 281	0.01517	0.0161
0.8	0.015	1.58	973 730	0.01517	0.0159
1	0.024	1.58	1,217,076	0.01517	0.0158
1.2	0.033	2.37	1,458,009	0.01517	0.0157
1.4	0.045	2.77	1 702 734	0.01517	0.0156
1.6	0.060	3.16	1,947,459	0.01517	0.0156
1.8	0.076	3.56	2 188 737	0.01517	0.0155
2	0.094	3.96	2 434 152	0.01517	0.0155
2.2	0.112	4.38	2,677,842	0.01517	0.0155
2.4	0.134	4.78	2 921 189	0.01517	0.0154
2.6	0.158	5.18	3 164 535	0.01517	0.0154
2.8	0.182	5.48	3 408 226	0.01517	0.0154
3	0.20	5.97	3 651 572	0.01517	0.0154

When calculating the resistance coefficient for different triples, using the dependence of the installation angle of the transfer pipe in Appendix 1, taking into account the installation angle of the transfer pipe for a micro hydropower plant, it can be seen that the resistance coefficient is equal to ξ - 0.6, and the value of the hydraulic resistance resulting from the deflection of the transfer pipe, calculated from equation (15), is presented in Figure 7.

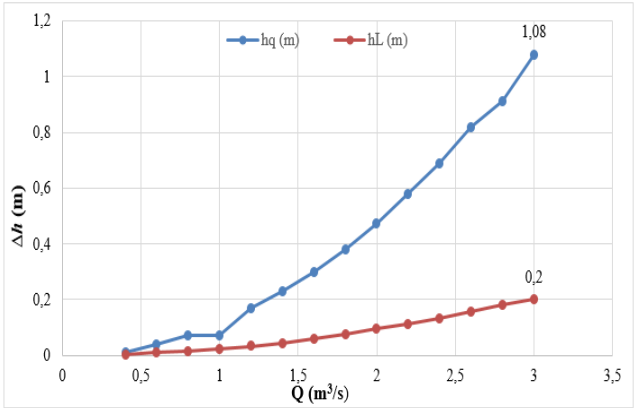


Figure 7. Total pressure loss in the transfer pipeline

As can be seen from Figure 7, for 3 m³/s, the pressure loss in the water path from the upper reservoir to the turbine was 0.20 m, and the head loss due to the hydraulic resistance created by the bend in the pipe was 1.08 m.

The calculated head for a micro hydroelectric power plant is calculated using the following equation 17:

$$H_n = h_m - \sum \Delta h \quad (17)$$

Here: H_n- head for micro hydropower plant, h_m- measured water pressure.

According to equation 17, the head for the micro hydropower plant was H_n-3.5 m and this is reflected in Figure 8.

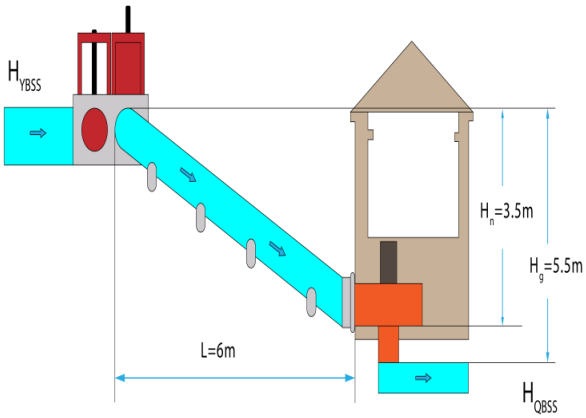


Figure 8. Head analysis for a micro hydropower plant.

The difference between the water level at the upper berm (the part of the reservoir in front of the dam) and the water level at the lower berm (the surface of the water source behind the dam) was 5.5 m (figure 4), and the pressure H_n from the upper berm to the turbine, minus the pressure loss in the water path in the transfer pipe (equation 17), was 3.5 m.

4. Discussion

The obtained results clearly show that head losses in micro hydropower systems increase with higher flow rates due to intensified turbulence and friction along the penstock. These outcomes are consistent with the theoretical predictions of the Darcy–Weisbach equation and earlier studies (Hashemi et al., 2020; Tian et al., 2013), which established a quadratic relationship between velocity and head loss. For example, at 3 m³/s, the observed head loss in the transfer pipeline was 0.20m, while hydraulic resistance at pipe bends contributed an additional 1.08 m. Such findings align with previous experimental and analytical investigations that emphasized the significant contribution of minor losses in real hydraulic systems.

Moreover, the pressure distribution results highlight that head stability is strongly influenced by pipeline geometry. At inlet sections, a sharp drop was observed, confirming earlier reports (Avci & Karagoz, 2019) on the sensitivity of entrance conditions to turbulence generation. In contrast, mid-pipe sections exhibited relatively stable pressure conditions, which can be considered favorable for turbine performance. The outlet section, however, demonstrated localized pressure increases under specific boundary conditions, suggesting the need for careful alignment of pipeline design with site-specific topography.

The broader implication of this study is the optimization of micro hydropower systems for rural electrification and agricultural applications. The findings support the hypothesis that careful modeling of hydraulic parameters not only improves turbine efficiency but also prevents risks of cavitation, system instability, and premature wear of structural components. In practice, selecting the appropriate pipe material, diameter, and surface roughness will reduce losses, as confirmed by roughness coefficient analyses in previous works (Rettore Neto et al., 2014; Jamil, 2019).

Future research should focus on extending these simulations to unsteady flow conditions and hybrid renewable systems. Additionally, the integration of smart monitoring tools with CFD-based predictive models could enhance real-time optimization of micro hydropower plants, ensuring both economic and environmental benefits.

5. Conclusions

This research demonstrates that head losses in micro hydropower systems are strongly dependent on flow rate, pipe diameter, and hydraulic resistance at bends. The results confirmed that as the flow rate increases from 1 to 3 m³/s, velocity and corresponding frictional head losses rise significantly, following the quadratic velocity–loss relationship. Moreover, the study revealed that pressure drop is greatest at pipe inlets and bends, which highlights the importance of optimizing pipe alignment and minimizing abrupt directional changes. It was also shown that the correct selection of pipe diameter and surface material can substantially reduce frictional resistance and improve overall system efficiency. With optimized parameters, micro hydropower plants can achieve greater operational stability, enhance turbine performance, and provide reliable renewable energy for remote areas. Overall, this study contributes to the field of hydropower engineering by integrating theoretical models with CFD simulations to better understand

hydraulic behavior in penstock systems, and the insights gained are essential for advancing sustainable micro hydropower technologies and ensuring their practical applicability in rural electrification projects.

References

1. A. Avci, I. Karagoz, A new explicit friction factor equation for laminar, transition and turbulent flows in smooth and rough pipes, European Journal of Mechanics - B/Fluids, Volume 78, 2019, Pages 182-187, ISSN 0997-7546,

2. https://doi.org/10.1016/j.euromechflu.2019.07.007

3. Hashemi, S., Filion, Y., Speight, V., & Long, A. (2020). Effect of pipe size and location on water-main head loss in water distribution systems. Journal of Water Resources Planning and Management, 146(6), 06020006.

4. Tian, X., Zhang, SXY, Valade, M., & Young, P. (2013). Head loss through pipefittings for laminar flows. Pipelines 2013: Pipelines and Trenchless Construction and Renewals—A Global Perspective, 301-308.

5. L.-J. Yang, V.-J. Joseph, N.-K. Unnam, and B. Esakki, "Design and Numerical Simulation of Biomimetic Structures to Capture Particles in a Microchannel," Fluids, vol. 7, no. 1, p. 32, Jan. 2022, doi: 10.3390/fluids7010032.

6. X. Guo, H. Cheng, H. Wang, Y. Cheng, and M. Sun, "Analysis of the Power Fluctuations Caused by the Unstable Flow in the Trifurcation of Multi-Turbine Diversion Systems with Common Penstock in Hydropower Units," Energies, vol. 12, no. 15, p. 2941, Jul. 2019, doi: 10.3390/en12152941.

7. 105. Pobitra Halder a, Arun Teja Doppalapudi b, Abul Kalam Azad b, M.M.K. KhanAdvances in Clean Energy Technologies 2021, 299-303 p

8. M. Irfan[1], Ermanu A H[2] and others. A design of electrical permanent magnet generator for rural area wind power plant, International Journal of Power Electronics and Drive System (IJPEDS) Vol. 9, No. 1, March 2018, pp. 269~275 ISSN: 2088-8694, DOI: 10.11591/ijpeds. v9n1.pp269-275.

9. Liangliang Wei,"Taketsune Nakamura , Keita Imai .Development and optimization of low-speed and high-efficiency permanent magnet generator for Mikro hydro-electrical generation system" Renewable Energy 147 (2020) 1653-1662..

10. Bilal Abdullah Nasir.Design of Micro-Hydro-Electric Power Station. International Journal of Advanced Technology and Engineering Exploration 2(5):39-47. January 2013

11. Bachrun, R., et al. "The effect of discharge on head loss with straight and bend flow directions in the pipeline." IOP Conference Series: Earth and Environmental Science. Vol. 841. No. 1. IOP Publishing, 2021.

12. Rettore Neto, O., Botrel, TA, Frizzone, JA, & Camargo, AP (2014). Method for determining friction head loss along elastic pipes. Irrigation Science, 32(5), 329-339. 2. SHICHIKHA, J. (2016). HEAD LOSS ANALYSIS IN PIPE FLOW SYSTEMS (Doctoral dissertation, University of Eldoret).

13. Jamil, R. (2019). Frictional head loss relation between Hazen-Williams and Darcy-Weisbach equations for various water supply pipe materials. International Journal of Water, 13(4), 333-347

14. De Souza Mendes, PR A Note on the Moody Diagram. Fluids, 9(4), 98. (2024). https://doi.org/10.3390/fluids9040098

15. Munson, B. R., Young, D. F., & Okiishi, T. H., Fundamentals of Fluid Mechanics, 4th Ed., New York: John Wiley and Sons, Inc, 2002. 568–570

16. Urishev, O., Salomov, U., Ergashev, S., Kuchkarov, A., Madaliev, M., Abdukarimov, B., & Juraev, N. (2025). Efficiency assessment of micro hydropower for agriculture using modern modeling. In BIO Web of Conferences (Vol. 173, p. 03031). EDP Sciences.

17. Urishev, O., Salomov, U., Ergashev, S., Kuchkarov, A., Madaliev, M., Abdukarimov, B., & Juraev, N. (2025). Efficiency assessment of micro hydropower for agriculture using modern modeling. In BIO Web of Conferences (Vol. 173, p. 03031). EDP Sciences.

Appendixs

Appendix 1

